Angiogenesis
https://doi.org/10.1007/s10456-020-09714-0

ORIGINAL PAPER

D-Peptide analogues of Boc-Phe-Leu-Phe-Leu-Phe-COOH induce neovascularization via endothelial *N*-formyl peptide receptor 3

Mohd I. Nawaz[1,5] · Sara Rezzola[1] · Chiara Tobia[1] · Daniela Coltrini[1] · Mirella Belleri[1] · Stefania Mitola[1] · Michela Corsini[1] · Annamaria Sandomenico[2] · Andrea Caporale[2,6] · Menotti Ruvo[2,3] · Marco Presta[1,4]

Received: 4 November 2019 / Accepted: 17 February 2020

Abstract

N-formyl peptide receptors (FPRs) are G protein-coupled receptors involved in the recruitment and activation of immune cells in response to pathogen-associated molecular patterns. Three FPRs have been identified in humans (FPR1–FPR3), characterized by different ligand properties, biological function and cellular distribution. Recent findings from our laboratory have shown that the peptide BOC-FLFLF (L-BOC2), related to the FPR antagonist BOC2, acts as an angiogenesis inhibitor by binding to various angiogenic growth factors, including vascular endothelial growth factor-A_{165} (VEGF). Here we show that the all-D-enantiomer of L-BOC2 (D-BOC2) is devoid of any VEGF antagonist activity. At variance, D-BOC2, as well as the D-FLFLF and succinimidyl (Succ)-D-FLFLF (D-Succ-F3) D-peptide variants, is endowed with a pro-angiogenic potential. In particular, the D-peptide D-Succ-F3 exerts a pro-angiogenic activity in a variety of in vitro assays on human umbilical vein endothelial cells (HUVECs) and in ex vivo and in vivo assays in chick and zebrafish embryos and adult mice. This activity is related to the capacity of D-Succ-F3 to bind FRP3 expressed by HUVECs. Indeed, the effects exerted by D-Succ-F3 on HUVECs are fully suppressed by the G protein-coupled receptor inhibitor pertussis toxin, the FPR2/FPR3 antagonist WRW4 and by an anti-FPR3 antibody. A similar inhibition was observed following WRW4-induced FPR3 desensitization in HUVECs. Finally, D-Succ-F3 prevented the binding of the anti-FPR3 antibody to the cell surface of HUVECs. In conclusion, our data demonstrate that the angiogenic activity of D-Succ-F3 is due to the engagement and activation of FPR3 expressed by endothelial cells, thus shedding a new light on the biological function of this chemoattractant receptor.

Keywords Angiogenesis · BOC2 · D-Peptide · Formyl peptide receptor · Huvecs

Introduction

N-formyl peptide receptors (FPRs) are implicated in the regulation of innate immune responses, inflammation and tissue repair [1]. They recognize peptides containing *N*-formylated methionine of bacterial and mitochondrial origin, as well as a variety of microbial non-formyl peptides, danger-associated molecular pattern host-derived peptides, small molecules and eicosanoids [1, 2].

Three FPRs have been identified in humans (FPR1–FPR3). They are characterized by different ligand properties, biological function and cellular distribution [3]. FPR1 and FPR2 are expressed by monocytes and neutrophils. In addition, FPR1 is expressed by microglial cells, astrocytes, hepatocytes and dendritic cells, whereas FPR2 can be found in a larger variety of non-myeloid cells [2]. Distinct from the other members of the FPR family, FPR3 (formerly named FPRL2) remains relatively poorly investigated.

Electronic supplementary material The online version of this article (https://doi.org/10.1007/s10456-020-09714-0) contains supplementary material, which is available to authorized users.

✉ Marco Presta
marco.presta@unibs.it

1 Department of Molecular and Translational Medicine, University of Brescia, Brescia, Italy

2 Istituto Di Biostrutture e Bioimmagini, CNR, Napoli, Italy

3 AnBition srl, Napoli, Italy

4 Italian Consortium for Biotechnology (CIB), Unit of Brescia, Trieste, Italy

5 Department of Ophthalmology, King Saud University, Riyadh, Kingdom of Saudi Arabia

6 Present Address: Istituto Di Cristallografia, CNR, Trieste, Italy

Published online: 09 March 2020

FPR3 is found in eosinophils, monocytes, macrophages and dendritic cells, but its functional role remains elusive [4]. A few FPR3 ligands have been identified, including F2L, an acetylated *N*-terminal fragment of human heme-binding protein [5], and the neuroprotective peptide humanin [6].

Endothelial cells have been shown to express FPRs [7–9] and scattered experimental evidence implicates FPRs in neovessel formation during inflammatory responses. For instance, the FPR ligands serum amyloid A (SAA), LL-37 and Hp(2–20) may regulate the angiogenic process under inflammatory conditions [1]. In addition, FPR activation appears to be involved in neovessel formation triggered by the vitreous fluid harvested from the eyes of patients affected by proliferative diabetic retinopathy [10]. In keeping with these observations, high levels of the FPR ligand SAA are detectable in vitreous and plasma of these patients [11] and in eyes with macular oedema [12, 13].

The peptide *N*-tert-butyloxycarbonyl (Boc)-Phe-D-Leu-Phe-D-Leu-Phe (BOC2) has been used extensively as a FPR1/FPR2 antagonist to assess the role of FPRs in physiological and pathological conditions (see [14–16] and references therein). Recent findings from our laboratory have shown that the BOC2-related peptide Boc-Phe-Leu-Phe-Leu-Phe (BOC-FLFLF in single letter code, L-BOC2) [17], having all-L configurations on its stereocenters, inhibits the angiogenic activity of various heparin-binding angiogenic growth factors, including vascular endothelial growth factor-A_{165} (VEGF), by interacting with their heparin-binding domain [9]. Thus, L-BOC2 appears to be endowed with a multi-heparin-binding growth factor antagonist activity, setting the basis for the design of novel L-BOC2-derived, multi-target angiogenesis modulators [9].

Peptides are gaining a renewed interest as potential drugs because of their generally high affinity and selectivity deriving from rapid adaptation on the surface of targets enabled by their structural flexibility. Thus far, more than 60 peptide drugs have been approved in the USA, Europe and Japan and even more peptides are under clinical development or have been tested in human clinical trials (reviewed in [18]). However, despite several advantages compared to low molecular weight organic therapeutics, short plasma half-life and negligible oral bioavailability may represent two major drawbacks intrinsic to the peptidic structure. The process of depeptidization, consisting in the systematic alteration of the peptidic scaffold to improve drug metabolism and pharmacokinetics features while retaining bioactivity is a major challenge in peptide-based therapeutics development because of the strong correlation between structure, conformation and biological properties of this class of molecules. Among the others, the inclusion of D-amino acids is a way to induce resistance to the activity of endogenous proteases, making D-peptide-based drugs more attractive and efficient than their L-peptide counterparts [19]. However, inversion of chiral centres in polypeptides might generate inactive variants or variants with chirally inverted specificities [20, 21]. Retro-inversion is more often applied to improve the stability of short bioactive all-L peptides, since this modification, when accompanied by reconstruction of the N- and C-terminal groups, generates new molecules with a formidable topological correlation, resulting from side chain spatial overlap with the parent one [22–24].

On this basis, we investigated the possibility that all-D peptide variants of L-BOC2 could represent VEGF antagonists more therapeutically relevant than their L-precursor. They included the D-enantiomer of L-BOC2 (Boc-D-FLFLF, from here on named D-BOC2), its D peptide derivative freed of the Boc group (D-FLFLF, from here on named D-F3) and a D peptide variant in which the Boc group was replaced by a succinimidyl moiety (succinyl-D-FLFL, from here on named D-Succ-F3). The structure of these peptides and of their all-L enantiomers are shown in Supplementary Fig. S1.

Surprisingly, we found that, at variance with its L-enantiomer, D-BOC2 is devoid of any VEGF antagonist activity. On the contrary, D-BOC2, as well as D-F3 and D-Succ-F3, are endowed with a significant pro-angiogenic capacity. In addition, we demonstrate that the angiogenic activity of D-Succ-F3 is due to the engagement and activation of FPR3 expressed by endothelial cells.

Materials and methods

Reagents

Reagents were from the following companies: M199, and RPMI-640 media, foetal calf serum (FCS) and SYBR Green PCR master mix (Gibco Life Technologies, Grand Island, NY, USA); porcine gelatin, endothelial cell growth factor, porcine heparin, 1-(mesitylene-2-sulfonyl)-3-nitro-1,2,4-triazole (MSNT), 1-methyl imidazole (MeIm), sym-collidine, succinic anhydride, *N*,*N*,diisopropylethylamine (DIPEA), tert-butyloxycarbonyl anhydride (Boc_2O), tetrahydrofuran (THF) and dimethylsulfoxide (DMSO) (Sigma-Aldrich, St. Louis, MO, USA); polyvinylpyrrolidone (PVP)-free polycarbonate filters (Costar, Cambridge, MA, USA); Diff-Quik (Dade-Behring, Milan, Italy); TRIzol Reagent, Moloney murine leukemia virus reverse transcriptase and anti-rabbit IgG Alexa Fluor 594 (Invitrogen, Carlsbad, CA, USA); anti-GAPDH and anti-Focal Adhesion Kinase (FAK) antibodies (Santa Cruz Biotechnologies, Santa Cruz, CA, USA); Matrigel (Cultrex BME, Gaithersburg, MD, USA); L-BOC2 (Phoenix Europe GmbH, Karlsruhe, Germany); anti-pVEGFR2 antibody (Cell Signaling Technology, Beverly, MA); anti-FPR1, anti-FPR2, anti-FPR3 and anti-FPR3(N-term) antibodies, and Trp-Arg-Trp-Trp-Trp-Trp-CONH(2) (WRW4) (Abcam, Cambridge, Great Britain);

anti-CD31 antibody and HRP-labelled anti-rabbit and anti-mouse polymers (Dako, Santa Clara, CA, USA); VEGFR2 kinase inhibitor SU5408 (MedChemExpress LLC, USA); VEGF-A_{165} (VEGF) was kindly provided by K. Ballmer-Hofer (PSI, Villigen, Switzerland); reagents for peptide synthesis, including resins, Fmoc-protected amino acids, couping agents 1-[Bis(dimethylamino)methylene]-1H-1,2,3-triazolo[4,5-b]pyridinium 3-oxid hexafluorophosphate (HATU), ethyl (hydroxyimino)cyanoacetate (Oxyma), *N*,*N*′-diisopropylcarbodiimide (DIC), trifluoroacetic acid (TFA) and the solvents dichloromethane (DCM) and dimethylformamide (DMF) (GL-Biochem, Shanghai, PRC; IRIS Biotech, Marktredwitz, Germany; Carlo Erba Reagents, Cornaredo, Italy); HPLC-grade CH_3CN (Romil, Dublin, Ireland).

Peptide synthesis

The peptides utilized in this study and their abbreviations are listed in Supplementary Table S1. The synthesis of the peptides was performed on a Wang Resin (loading 0.79 mmol/g) using the Fmoc solid-phase strategy. Resins (150 mg, 118.5 µmol) were swollen in DCM for 1 h, then the first amino acid was introduced by treatment with Fmoc-Phe-OH or Fmoc-D-Phe-OH (5 eq)/MSNT (5.0 eq)/MeIm (3.5 eq) in DCM for 3 h and repeated overnight. Resin loading was assessed according to standard procedures [25] and was estimated to be 0.65 mmol/g. Fmoc deprotection of the first amino acid was performed with a piperidine solution at 40% in DMF for 5 min and at 20% for 10 min. Each amino acid (4.0 eq) was double-coupled using 0.5 M Oxyma, 0.5 M DIC in DMF, for 30 min in the first coupling and 0.5 M HATU and 2.0 M sym-collidine in DMF for 30 min in the second coupling [26]. Coupling efficiency was assessed by Kaiser test. Each step was followed by resin washing (3 × 5 min) with DMF. *N*-terminal succinimidyl peptides (L-Succ-F3 and D-Succ-F3) were generated on resin after chain assembly by treatment for 30 min with a solution of succinic anhydride (10 eq) in DMF, containing 5% (v/v) DIPEA. Peptides were cleaved from the resins by treatment for 4 h with a freshly prepared TFA/H_2O solution (95:5, v/v). TFA was evaporated under a mild nitrogen stream; peptides were dissolved in H_2O/CH_3CN (75:25, v/v) and lyophilized. Boc-protected peptides (L-BOC2 and D-BOC2) were obtained from the corresponding unprotected crude L-F3 and D-F3 by treatment in solution with Boc_2O. Peptides were dissolved in 1.0 M $NaHCO_3$ (10 mL) and a solution of Boc_2O (1.2 eq) in THF (10 mL) was added dropwise for 30 min. The reaction mixture was stirred at room temperature overnight. The solution was acidified at pH 3.0 with 1.0 M HCl and dried under vacuum. Peptides were purified on a preparative WATERS 2545 Quaternary Gradient Module HPLC (Waters, Milan, Italy) supplied with a WATERS 2489 UV/visible Detector, using a XBRIDGE Prep BEH130 OBDTM C18 column (5 µm, 50 × 19 mm ID). A gradient from 20 to 70% of solvent B in solvent A over 10 min at a 10 mL/min flow rate was used to purify the peptides. Solvent A was 0.1% TFA in H_2O; solvent B was 0.1% TFA in CH_3CN. Purified peptides were characterized for purity and identity by an Agilent 1290 Infinity LC System coupled to an Agilent 6230 time-of-flight (TOF) MS System (Agilent Technologies, Cernusco Sul Naviglio, Italy), using a C18 Waters xBridge (3 µm, 50 × 4.6 mm) column, applying a linear gradient from 30 to 95% of 0.05% TFA in CH_3CN over 15 min at a flow rate of 0.2 mL/min. Yields of purified peptides ranged between 65 and 75%. Peptides were > 99% pure and their MWs were consistent with the calculated masses within the limits of the experimental error (see Supplementary Table S1).

Cell cultures

Human umbilical vein endothelial cells (HUVECs) were isolated from umbilical cords as described [27]. Routinely, cells were used at early (I–IV) passages. Cells were grown on culture plates coated with porcine gelatin in M199 medium supplemented with 20% FCS, endothelial cell growth factor (10 µg/mL), and porcine heparin (100 µg/mL). Human THP-1 monocytic cells (ATCC® TIB-202™) and human Jurkat leukemia cells (ATCC) were provided by S. Sozzani (University of Brescia, Italy) and grown in RPMI-1640 medium *plus* 10% FCS. Cells were tested regularly for Mycoplasma negativity.

Western blot analysis

Cells were collected and washed in cold PBS and homogenized in lysis buffer containing 1% Triton-X100, 0.1% polyethylene glycol dodecyl ether (BRIJ), 1.0 mM sodium orthovanadate, and protease inhibitors cocktail. The cell lysate was centrifuged, and the supernatant was collected. Aliquots of each sample containing equal amounts of protein (20–50 µg) were subjected to SDS-PAGE. Gels were transblotted onto PVDF membrane and blots were blocked with 3.0% BSA in PBS for 1 h at room temperature. The blotting analysis was performed with anti-pVEGFR2, anti-FPR1, anti-FPR2, or anti-FPR3 antibodies. After treating the membranes with appropriate secondary horseradish peroxidase-labelled secondary antibody, blots were developed with enhanced chemiluminescence reagent (Bio-rad Laboratories, Inc. Hercules, CA). Images were acquired (ChemiDoc Touch; Bio-Rad Laboratories, Inc.), and band intensity was evaluated (Image Lab 3.0 software; Bio-Rad Laboratories, Inc.). Data were normalized to the levels of GAPDH or FAK expression.

Fluorescence-activated cell sorting (FACS) analysis

For the FACS analysis of FPR1-3 protein expression in HUVECs, cells were resuspended in MACS buffer containing 1.0% FCS and incubated for 30 min at 4 °C with 1:100 dilution of anti-FPR1, anti-FPR2, or anti-FPR3 antibody. Then, cells were washed, incubated with Alexa Fluor 647 anti-rabbit secondary antibody for 20 min at 4 °C and analysed with a MACSQuant cytofluorimeter (Milteny Biotec) using FlowJo software. For the competition binding assay, cells were incubated with anti-FPR3 antibody in the absence or presence of 1.2 mM D-Succ-F3 peptide or 0.5 mM WRW4. For FPR3 desensitization experiments, HUVECs were preincubated with 30 µM WRW4 for 48 h before FACS analysis.

Real-time PCR

Steady-state transcription levels of *FPR1*, *FPR2*, *FPR3*, and *GAPDH* genes were evaluated in THP1 cells and HUVECs isolated from different donors by semi-quantitative real-time PCR (RT-PCR). The expression levels of murine endothelial *Cd31* and pan-leucocyte *Cd45* markers were determined in harvested Matrigel plugs by quantitative RT-PCR (RT-qPCR) as described [28]. Briefly, total RNA was extracted using TRIzol reagent according to manufacturer's instructions (Invitrogen, Carlsbad, CA). Contaminating DNA was digested using DNAse (Promega) and 2.0 µg of total RNA were retro-transcribed with MMLV reverse transcriptase (Invitrogen) using random hexaprimers in a final volume of 20 µL. Then, 1/10th of the reaction product of semi-quantitative RT-PCR was analysed on the agarose gel. RT-qPCR was performed with a ViiA™ 7 Real-Time PCR Detection System (Applied Biosystems) using iQ™ SYBR Green Supermix (Biorad) according to the manufacturer's instructions. Primer sequences for the genes of interest are listed in Supplementary Table S2.

HUVEC sprouting assay

HUVEC aggregates (800 cells/spheroid) embedded in fibrin gel [29] were treated with VEGF and increasing concentrations of the peptide under test. DMSO was used as a control unless specified otherwise. Sprouts were counted after 24 h and data were expressed as a fold change vs control.

Matrigel morphogenesis assay

The assay was performed as described [30]. Briefly, 10 µL of Matrigel were added to the wells of a 15-well plate (IBIDI) and allowed to solidify for 30 min at 37 °C. Then, 1.0×10^4 HUVECs resuspended in 50 µL of M199 medium *plus* 5% FCS were seeded on the top of the Matrigel in the presence of DMSO, VEGF or D-Succ-F3. After 6 h of incubation, the formation of angiogenic meshes was evaluated under an inverted microscope.

HUVEC chemotaxis assay

HUVECs (1.0×10^6 cells/mL) resuspended in M199 medium *plus* 2.0% FCS were seeded in the upper compartment of a Boyden chamber containing 0.1% gelatin-coated PVP-free polycarbonate filters (8.0 µm pore size). D-Succ-F3 diluted in M199 medium *plus* 2.0% FCS, or HUVEC complete medium [31] were placed in the lower compartment. When indicated, cells were co-incubated for 30 min with the anti-FPR3 antibody and then seeded in the upper compartment. After 4 h of incubation, cells migrated to the lower side of the filter were fixed with methanol and stained with Diff-Quik. The number of migrated cells was determined by counting five microscopic fields per well for each sample in triplicate.

HUVEC proliferation assay

HUVECs were seeded at 1.7×10^4 cells/cm^2 and serum starved overnight. Then, cells were stimulated with 30 ng/mL VEGF or increasing concentrations of D-Succ-F3. After 48 h, cells were counted with a MACSQuant cytofluorimeter.

HUVEC survival assay

HUVECs were maintained overnight in complete medium or in M199 medium *plus* 2.5% FCS in the absence or in the presence of increasing concentrations of D-Succ-F3. Apoptotic cell death was assessed by Annexin-V/Iodide Propidium double staining (Immunostep) according to the manufacturer's instructions.

Ex vivo *murine aorta ring assay*

The assay was performed as described [32]. Briefly, 1.0-mm mice aorta rings embedded in fibrin gel were incubated with increasing concentrations of L-Succ-F3 or D-Succ-F3 in serum-free endothelial cell basal medium (Clonetics). After 5 days, vessel sprouts, morphologically distinguishable from scattering fibroblasts/smooth muscle cells, were counted under a stereomicroscope.

Chick embryo chorioallantoic membrane (CAM) assay

Alginate beads (4.0 µL) containing DMSO or D-Succ-F3 (8.0–150 ng/pellet) were placed on the top of the CAM of fertilized white Leghorn chicken eggs at day 11 of incubation (7 eggs per experimental point) [33]. Pellets loaded with

VEGF (0.1 µg/pellet) were used as a positive control. After 3 days, newly formed microvessels converging toward the implant were counted under a stereomicroscope (STEMI-SR, Zeiss) at × 5 magnification.

Zebrafish yolk membrane (ZFYM) angiogenesis assay

Zebrafish (Danio *rerio*) adults (wild type AB strain) were maintained at 28 °C on a 14 h light/10 h dark cycle under standard laboratory conditions [34]. Embryos at 48 hpf were anesthetized with 0.016% tricaine and injected into the perivitelline space with 0.04% DMSO or increasing concentrations of D-Succ-F3 in the proximity of developing subintestinal vein vessels using an InjectMan IN2 microinjector (Eppendorf) equipped with FemtoJet. The angiogenic response was evaluated at 72 hpf after alkaline phosphatase (AP) staining [35]. The total number of ectopic AP^+ vessels sprouting from the SIVs on both sides of the embryo body was manually counted in each embryo ($n = 41$ in two independent experiments). Representative images were acquired using a Leica MZ16F stereomicroscope equipped with a QI ClicK Mono Uncooled Camera and Qcapture Pro software.

In vivo *Matrigel plug assay*

Matrigel was mixed at 4 °C with DMSO or with 5.0 µg of D-Succ-F3 or L-Succ-F3 and injected subcutaneously (0.3 mL/mouse) into the flank of 6–8 week-old C57BL6 female mice (Charles River, Calco, Italy). After 7 days, plugs were harvested and processed for total RNA extraction after adding to each plug a fixed number of human cells as an internal standard [28]. Then, total RNA was extracted using the TRIzol Reagent, samples were analysed for the expression of murine *Cd31* and *Cd45* markers by RT-qPCR and data were normalized for human *GAPDH* expression levels [28]. In each experiment, an arbitrary value equal to 1.0 was assigned to the levels of expression of the gene(s) measured in one DMSO Matrigel sample that was used as a reference.

Immunohistochemistry

Human umbilical cord fragments were formalin fixed and paraffin embedded. Serial sections (7 µm) were dewaxed, hydrated, and processed for immunohistochemistry with rabbit anti-human FPR3 (N-terminal) and mouse anti-human CD31 antibodies. After incubation with Envision HRP-labelled anti-rabbit or anti-mouse polymer, positive signal was revealed by 3,3′-diaminibenzidine staining. Sections were counterstained with Mayer's hematoxylin and images were acquired with a Zeiss Axioplan 2 microscope at 20 × magnification.

Statistical analysis

Statistical analysis was performed with GraphPad Prism 6 (San Diego, CA, USA) using Student's *t*-test or one-way analysis of variance followed by Bonferroni multiple comparison post test. All data are the mean ± SEM of three experiments unless specified otherwise and p values < 0.05 were considered statistically significant.

Results

L-BOC2-derived D-peptides induce HUVEC sprouting

Previous observations had shown the capacity of L-BOC2 to inhibit the angiogenic activity of VEGF [9]. On this basis, its D-enantiomer D-BOC2 (Supplementary Table S1) was synthesized in the attempt to improve the stability and possibly the activity of the precursor molecule. Then both molecules were assessed for their capacity to affect the pro-angiogenic activity exerted by VEGF on HUVEC spheroids embedded in a 3D fibrin gel [29]. As anticipated, L-BOC2 inhibits the sprouting of HUVEC spheroids mediated by VEGF in a dose-dependent manner, with no effect when administered in the absence of VEGF. At variance, its all-D variant D-BOC2 did not exert any inhibitory effect on VEGF activity. On the contrary, D-BOC2 was able to induce the sprouting of HUVEC spheroids and to exert an additive pro-angiogenic effect when administered to endothelial cells in the presence of a fixed amount of VEGF (Fig. 1a). Unexpectedly, these data suggest that the replacement of L-amino acids by their D-enantiomers induced extensive structural modifications that abolished the VEGF antagonist activity of the peptide and conferred a pro-angiogenic potential to the D-enantiomer D-BOC2.

In order to confirm these preliminary observations and to elucidate the contribution of the N-terminal Boc group to the observed pro-angiogenic activity of the all-D derivative, the D-peptide D-F3 lacking the N-terminal Boc protecting group was tested in the HUVEC spheroid assay. In parallel, we also tested the D-Succ-F3 peptide in which the Boc group at the N-terminus of the molecule was replaced by a succinic acid moiety in order to achieve a pseudo-symmetrical compound with the potential ability to interact with its target(s) in two similar orientations, with a possible improved activity. The corresponding L-enantiomers L-F3 and L-Succ-F3 (Supplementary Table S1) were used as controls. In keeping with the results obtained with D-BOC2, both D-F3 and D-Succ-F3 induced the sprouting of HUVEC spheroids, whereas their all-L variants were inactive (Fig. 1b). Thus, the pro-angiogenic activity of these D-FLFLF peptides appears to be independent of the presence or chemical nature of their *N*-terminal moiety, but is strictly dependent on the

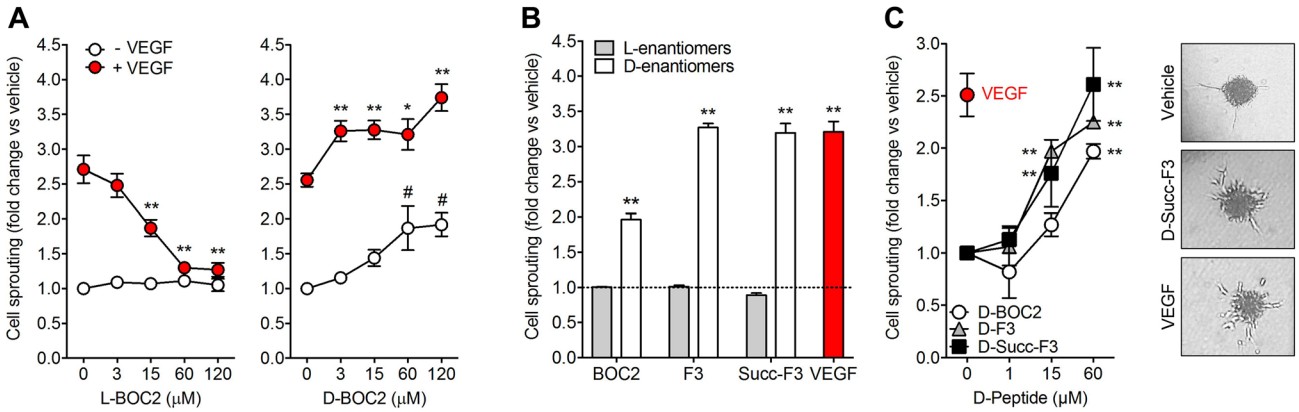

Fig. 1 L-BOC2 and D-BOC2 derivatives exert a different biological activity in HUVECs. **a** HUVEC spheroids embedded in 3D fibrin gel were treated with vehicle or 30 ng/mL VEGF in the absence or in the presence of the indicated concentrations of L-BOC2 (left panel) or D-BOC2 (right panel). $^{**}p<0.01$ vs VEGF alone; $^{\#}p<0.01$ vs vehicle. **b** HUVEC spheroids were treated with vehicle (dashed line), 30 ng/mL VEGF or the L- or D-enantiomers of BOC2 and F3 or Succ-F3 peptides, all at 60 μM final concentration. $^{**}p<0.01$ vs vehicle. **c** HUVEC spheroids were treated with 30 ng/mL VEGF or the indicated concentrations of D-BOC2, D-F3, or D-Succ-F3. $^{**}p<0.01$ vs vehicle. Representative images of HUVEC spheroids treated with DMSO, 60 μM D-Succ-F3 or 30 ng/mL VEGF are shown in the right panels. For all the experiments, radially growing endothelial sprouts were counted after 24 h of incubation and data (mean ± SEM of three independent experiments) were expressed as fold change vs vehicle

conformation induced by the presence of the D-residues. In particular, dose–response experiments indicated that D-F3 and D-Succ-F3 were able to induce a response in HUVECs similar to that exerted by an optimal concentration of VEGF, whereas the L-variants were ineffective (Fig. 1c). On this basis, D-Succ-F3 was used in all the following experiments due to its higher biological activity compared to D-BOC2 and its better solubility profile compared to D-F3.

In keeping with the lack of anti-VEGF activity shown by D-BOC2, D-Succ-F3 did not affect VEGFR2 phosphorylation triggered by VEGF in HUVECs and exerted an additive effect on the sprouting of HUVEC spheroids when co-administered with the growth factor (Supplementary Fig. S2A, B). Notably, the capacity of D-Succ-F3 to induce HUVEC sprouting was not affected by the tyrosine kinase VEGFR inhibitor SU5408 [36] (Supplementary Fig. S2C). Accordingly, when compared to VEGF, administration of D-Succ-F3 alone was unable to trigger VEGFR2 phosphorylation in endothelial cells (Supplementary Fig. S2D). Thus, the pro-angiogenic activity of D-Succ-F3 appears to be independent of the VEGF/VEGFR2 axis.

The D-Succ-F3 peptide triggers angiogenic responses in vitro and in vivo

In order to confirm the pro-angiogenic potential of D-Succ-F3, we tested its capacity to exert morphogenic and chemotactic responses in HUVECs seeded on Matrigel or gelatin, respectively. As shown in Fig. 2a, b, D-Succ-F3 induces capillary-like morphogenesis in HUVECs seeded on Matrigel and their migration through a gelatin-coated filter in a Boyden chamber assay. The response was similar to that exerted by an optimal dose of VEGF or by HUVEC complete medium that were used as positive controls in the two assays, respectively. Accordingly, D-Succ-F3 induced a significant increase in the formation of endothelial cell sprouts in an ex vivo murine aorta ring assay. When tested under the same experimental conditions, L-Succ-F3 was ineffective, thus confirming the specificity of the effect deriving from the peculiar all-D peptide structure (Fig. 2c). Notably, the D-peptide was unable to trigger a significant proliferative response or to support cell survival in HUVECs (Supplementary Fig. S3).

In keeping with its pro-angiogenic ability, alginate beads containing 150 ng/pellet of D-Succ-F3 induced a potent neovascular response when placed on the top of the chick embryo CAM similar to that exerted by an optimal dose of VEGF (100 ng/pellet, [37]) (Fig. 2d).

Next, the capacity of D-Succ-F3 to stimulate neovessel formation was assessed in vivo in the ZFYM angiogenesis assay [35]. As shown in Fig. 2E, 12–50 pg/embryo of D-Succ-F3 injected into the perivitelline space of zebrafish embryos caused the sprouting of subintestinal vein vessels in a dose-dependent manner, with a maximal effect at the

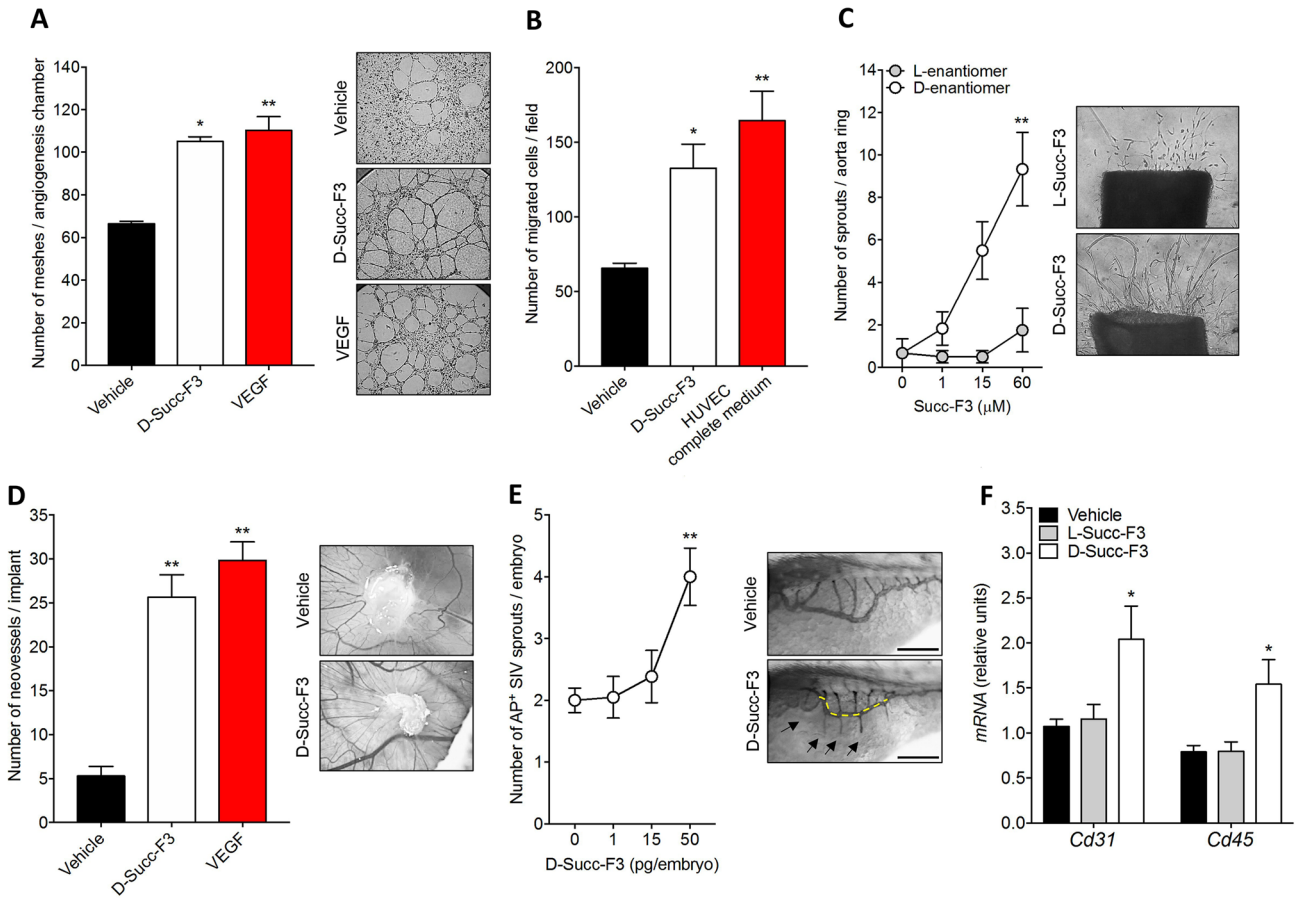

Fig. 2 Pro-angiogenic activity of D-Succ-F3. **a** HUVEC morphogenesis assay. HUVECs were seeded on Matrigel in the presence of vehicle, 60 µM D-Succ-F3 or 30 ng/mL VEGF. Angiogenic meshes was counted after 6 h of incubation and data (mean ± SEM of four independent experiments) were expressed as the number of meshes per field. Representative images of HUVEC morphogenesis on Matrigel following the different treatments are shown in the right panels. **b** HUVEC migration assay. Cells were seeded in the upper compartment of a Boyden chamber, whereas vehicle, 60 µM D-Succ-F3, or HUVEC complete medium were placed in the lower compartment. Migrated cells were counted after 4 h of incubation and data were expressed as the number of migrated cells per field (mean ± SEM of three independent experiments). **c** Murine aorta ring assay. Murine aorta rings were embedded in the 3D-fibrin gel and treated with L-Succ-F3 or D-Succ-F3. After 5 days, vessel sprouts were counted under a stereomicroscope and data were expressed as the number of sprouts per aorta ring (mean ± SEM of two independent experiments). Representative images of aorta rings treated with the two compounds (60 µM) are shown in the right panels. **d** Chick embryo CAM assay. Alginate beads containing vehicle, 150 ng D-Succ-F3, or 100 ng VEGF were placed on the top of the CAM at day 11 of incubation. Newly formed vessels converging toward the implant were counted after 3 days (mean ± SEM of three independent experiments). Representative images of CAMs grafted with vehicle or D-Succ-F3 are shown in the right panels. **e** ZFYM angiogenesis assay. Two nL of 0.04% DMSO or of the indicated concentrations of D-Succ-F3 were injected into the perivitelline space of zebrafish embryos at 48 hpf. The angiogenic response was evaluated at 72 hpf following alkaline phosphatase (AP) staining. Data are represented as a total number of ectopic AP^+ SIV sprouts/embryo (mean ± SEM of 41 embryos in two independent experiments). Representative images of the formation of ectopic SIVs (arrows) in embryos treated with vehicle or 50 pg D-Succ-F3. Scale bar: 200 µm. **f** Matrigel plug angiogenesis assay. Matrigel plugs containing vehicle and 5.0 µg of L-Succ-F3 or of D-Succ-F3 were injected in the flank of female mice. After 7 days, quantification of the expression of endothelial cell *Cd31* and leukocyte *Cd45* markers was performed by RT-qPCR in harvested plugs. Data are mean ± SEM of three experiments ($n = 5$–10 mice for each experiment) and are expressed as *Cd31*/*GAPDH* and *Cd45*/*GAPDH* mRNA ratios. *$p < 0.05$ or **$p < 0.01$ vs vehicle

dose of 50 pg/embryo. Finally, to get further insights about the D-Succ-F3-driven neovascular response, D-Succ-F3 was embedded in Matrigel and implanted subcutaneously in mice. RT-qPCR analysis of the plugs harvested 7 days after implantation demonstrated a significant increase of the expression of the endothelial marker *Cd31* and of the pan-leukocyte marker *Cd45* in D-Succ-F3 plugs when compared to vehicle- or L-Succ-F3-loaded plugs (Fig. 2f).

Together, these data demonstrate the capacity of D-Succ-F3 to act as a pro-angiogenic compound in vitro and in vivo.

FPR3 mediates the biological activity of D-Succ-F3 in HUVECs

The strong structural correlation between L-BOC2 and its all-D variants led to the hypothesis that the angiogenic activity shown by D-Succ-F3 might be related to its capacity to interact with FPRs expressed by HUVECs.

Previous observations had described the expression of FPR2 in HUVECs, with no information about the expression of the other members of the FPR family in these cells [7, 8]. On the other hand, preliminary data from our laboratory had identified FPR3 as the only receptor expressed by HUVECs [9]. On this basis, RT-PCR analysis was performed to assess the levels of *FPR1*, *FPR2* and *FPR3* transcripts in 5 independent HUVEC preparations established from healthy donors. When tested at the first cell passage, all HUVEC preparations express *FPR3*, but not *FPR1* and *FPR2*, whereas monocytic THP-1 cells express all three *FPR* genes (Fig. 3a). Similar results were obtained when HUVECs were analysed up to the fourth cell passage (data not shown). FACS analysis confirmed the expression of FPR3 protein on the cell surface of our primary HUVEC cultures, whereas FPR1 and FPR2 were undetectable (Fig. 3b, c). When HUVEC lysates were analysed by Western blotting, the same anti-FPR3 antibody used for FACS analysis recognized an immunoreactive band that migrated with the predicted apparent molecular weight, identical to that

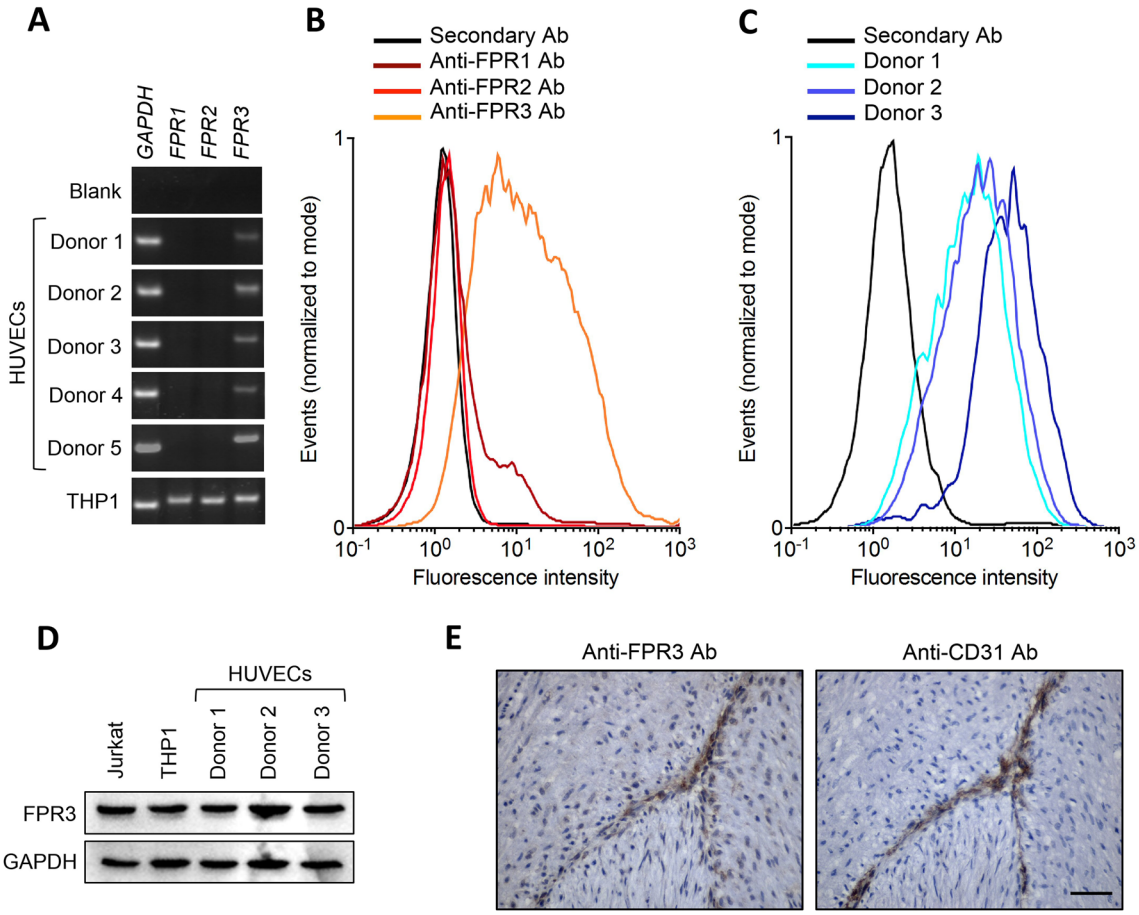

Fig. 3 HUVECs express *N*-Formyl Peptide Receptor 3. **a** HUVECs were isolated from five donors and the expression levels of *FPR1*, *FPR2*, and *FPR3* transcripts were evaluated by semi-quantitative RT-PCR in parallel with a human monocytic THP-1 cell extract here used as positive control. Similar results were obtained when HUVEC cultures were tested at I–IV cell passage (not shown). **b** HUVEC preparation from Donor 5 was assessed for the expression of cell surface FPR1, FPR2, and FPR3 proteins by FACS analysis. **c** HUVEC preparations from Donors 1–3 were assessed for the expression of cell surface FPR3 protein by FACS analysis. **d** Total FPR3 protein levels in the extracts of HUVEC preparations were evaluated by Western blot analysis. THP-1 and Jurkat cell extracts were used as positive controls. **e** Immunohistochemical analysis of human umbilical vein. Paraffin-embedded serial sections of an isolated human umbilical vein were immunostained with anti-FPR3 or anti-CD31 antibodies. Endothelial cells express both antigens. No immunoreactivity was observed in the absence of the primary antibody (not shown). Scale bar = 50 μm

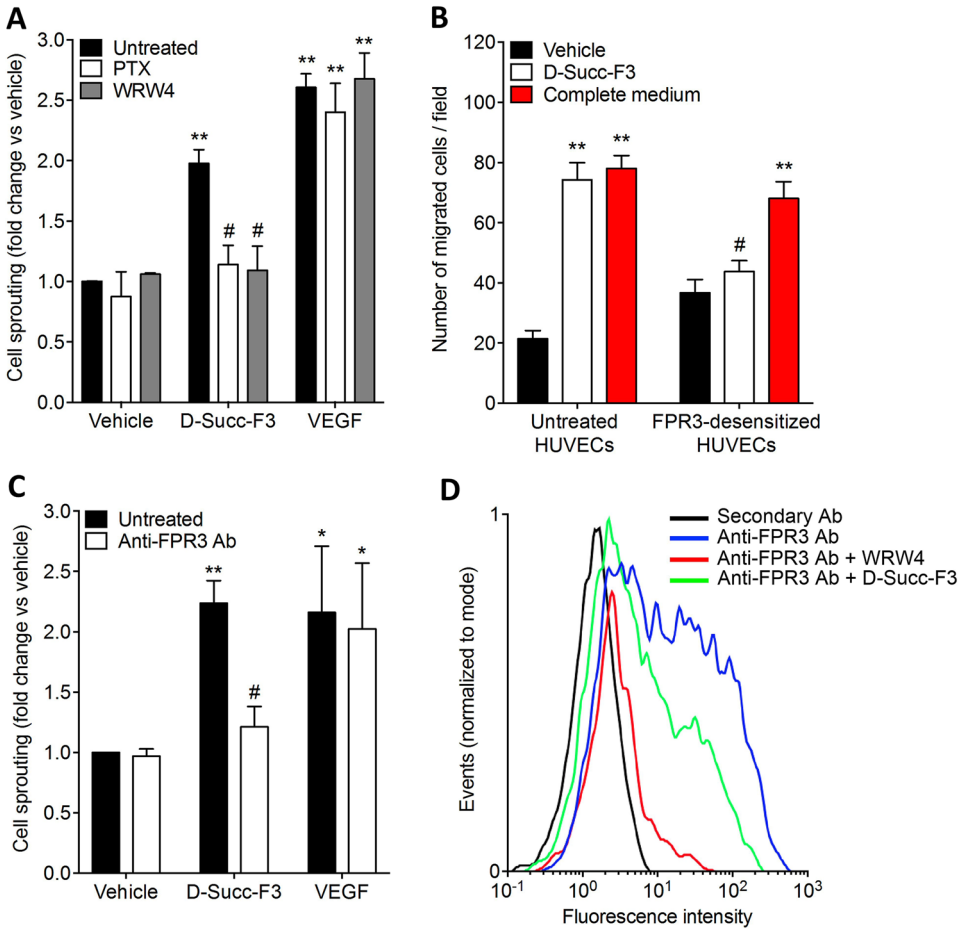

Fig. 4 FPR3 mediates the biological activity of D-Succ-F3 in HUVECs. **a** HUVEC sprouting assay. HUVEC spheroids were treated with vehicle or with 100 ng/mL pertussis toxin (PTX) or 50 μM WRW4 in the absence or in the presence of 30 μM D-Succ-F3 or 30 ng/mL VEGF. Radially growing endothelial sprouts were counted after 24 h of incubation and data (mean ± SEM of three independent experiments) were expressed as fold change vs vehicle. **b** HUVEC migration assay. Untreated and FPR3-desensitized HUVECs were seeded in the upper compartment of a Boyden chamber, whereas vehicle, 60 μM D-Succ-F3 or HUVEC complete medium were placed in the lower compartment. Migrated cells were counted after 4 h of incubation and data were expressed as the number of migrated cells per field (mean ± SEM of three independent experiments). **c** HUVEC spheroids were treated with vehicle, 30 μM D-Succ-F3 or 30 ng/mL VEGF in the absence or in the presence of an anti-FPR3 antibody (1:100 dilution, vol:vol). Radially growing endothelial sprouts were counted after 24 h of incubation and data (mean ± SEM of three independent experiments) were expressed as fold change vs vehicle. **d** HUVECs (1.0×10^4/100 μL) were incubated for 30 min at 4 °C with vehicle (blue line), 1.0 mM WRW4 (red line) or 0.5 mM D-Succ-F3 (green line) in MACS buffer. Then, cells were evaluated for the capacity to bind the anti-FPR3 antibody by FACS analysis. Omission of the primary antibody represented the negative control (black line). $^*p < 0.05$ or $^{**}p < 0.01$ vs vehicle; $^{\#}p < 0.01$ vs D-Succ-F3 alone

observed for THP-1 and lymphoblastic Jurkat cell extracts, here used as positive controls (Fig. 3d). Accordingly, immunohistochemical analysis performed with a distinct anti-FPR3 antibody, demonstrated that FPR3 is expressed in vivo by $CD31^+$ endothelial cells in human umbilical cord blood specimens (Fig. 3e). Together, these observations unambiguously identify FPR3 as the only detectable member of the FPR family expressed by HUVECs under our experimental conditions.

As shown in Fig. 4a, the G protein-coupled receptor inhibitor pertussis toxin hampers the capacity of D-Succ-F3 to induce the sprouting of HUVEC spheroids with no effect on VEGF activity, thus supporting the hypothesis that the activity of D-Succ-F3 is mediated by G protein-coupled FPRs. Accordingly, the FPR2/FPR3 antagonist WRW4 [38, 39] abrogated the activity of D-Succ-F3 (Fig. 4a). These data, together with the observation that HUVECs express FPR3, but not the other members of the FPR family, implicate FPR3 in mediating the pro-angiogenic activity of D-Succ-F3 in HUVECs by a mechanism that involves the binding site of the FPR inhibitor WRW4.

To further substantiate this hypothesis, HUVECs were pre-incubated for 48 h with WRW4, thus leading to desensitization and downregulation of FPR3 receptors on the

cell surface [4] (Supplementary Fig. S4). As anticipated, FPR3 desensitization caused a decrease in the capacity of HUVECs to migrate in response to D-Succ-F3 in a Boyden chamber assay, with no effect on the migration induced by the complete HUVEC medium here used as a positive control (Fig. 4b). Accordingly, the anti-FPR3 antibody hampered the capacity of D-Succ-F3 to induce the sprouting of HUVEC spheroids with no effect on VEGF activity (Fig. 4c). Conversely, similar to WRW4, D-Succ-3 prevented the binding of the anti-FPR3 antibody to the surface of HUVECs as assessed by FACS analysis (Fig. 4d).

Together, these observations provide experimental evidence about the role of FPR3 in mediating the pro-angiogenic activity of D-Succ-F3 in HUVECs.

Discussion

The present work stemmed from the observation that the L-BOC2 peptide, structurally related to the FPR inhibitor BOC2 [14], is endowed with an angiosuppressive potential due to its capacity to bind VEGF, as well as a variety of other heparin-binding pro-angiogenic mediators, setting the basis for the design of novel multi-target angiogenesis inhibitors [9].

In this frame, given the higher stability of D-peptides when compared to their L-enantiomers, we investigated the possibility that D-BOC2, the D-mirror image of L-BOC2, might represent an interesting anti-angiogenic compound. Surprisingly, we found that D-BOC2 was devoid of any VEGF antagonist activity. On the contrary, D-BOC2 showed a significant pro-angiogenic potential when tested in a HUVEC sprouting assay. Similar results were obtained with the D-peptides D-F3 and D-Succ-F3 that share with D-BOC2 the same D-amino acid sequence. Accordingly, the D-peptide D-Succ-F3 exerts a pro-angiogenic activity in a variety of in vitro assays on HUVECs and in ex vivo and in vivo assays in chick and zebrafish embryos and adult mice.

Given the above-mentioned role of FPRs in angiogenesis and the capacity of BOC2 and related peptides to exert FPR agonist/antagonist activities [14–16, 40, 41], we addressed the possibility that Succ-D-F3 may exert its pro-angiogenic activity by interacting with FPRs on the endothelial cell surface. Three FPRs have been identified in humans (FPR1–FPR3), characterized by different ligand properties, biological function and cellular distribution [3]. Among them, FPR3 has been poorly investigated and its functional role is uncertain [4].

Even though previous observations had shown the expression of FPR2 in HUVECs, no data were available about FPR3 expression in these cells [7, 8]. At variance, preliminary data from our laboratory had identified FPR3 as the only member of the FPR family expressed by HUVECs [9]. In the present work, we confirmed and extended these preliminary findings by showing that FPR3 is expressed in HUVECs at both transcript and protein levels, as demonstrated by RT-PCR, FACS and Western blot analyses. In contrast, FPR1 and FPR2 expression were below the limits of detection in our cells. These findings were confirmed on five independent HUVEC preparations from distinct donors, with no significant differences between primary cell isolates and HUVECs maintained in culture up to the fourth cell passage. Accordingly, immunohistochemical analysis demonstrated that HUVECs express FPR3 in vivo. Together, these observations unambiguously identify FPR3 as the only member of the FPR family expressed by HUVECs under our experimental conditions. Further experiments will be required to investigate how cell origin and experimental conditions may affect the expression of different FPRs in endothelial cells.

Several experimental evidences support the involvement of FPR3 in endothelial stimulation by D-Succ-F3. Indeed, the effects exerted by D-Succ-F3 on HUVECs are fully suppressed by the G protein-coupled receptor inhibitor pertussis toxin, the FPR2/FPR3 antagonist WRW4 and by an anti-FPR3 antibody. A similar inhibition was observed following WRW4-induced FPR3 desensitization in HUVECs. Finally, D-Succ-F3 prevented the binding of the anti-FPR3 antibody to the cell surface of HUVECs. Together, these results show that FPR3 expressed by HUVECs mediates the angiogenic activity of D-Succ-F3. Clearly, we can not rule out the possibility that D-Succ-F3 may interact also with other members of the FPR family to exert its pro-angiogenic action. In particular, further studies will be required to identify the FPR orthologues responsible for the neovascular responses elicited by D-Succ-F3 in zebrafish and chick embryos, as well as in adult mice.

A few natural FPR3 ligands have been identified, including F2L [5] and humanin [6], that can bind also FPR2 although with different potency [5, 6]. Notably, both F2L and humanin modulate the angiogenic process even though with opposite effects. F2L, a proteolytic fragment of the heme-binding protein originally identified as an endogenous ligand for FPR3 [5], induces the chemotactic migration of HUVECs, which is inhibited by the FPR2/FPR3 antagonist WRW4 [40]. In apparent contradiction with these observations, F2L inhibits HUVEC proliferation and tube formation triggered by the human cathelicidin antimicrobial peptide LL-37/hCAP-18 [40], a pro-angiogenic FPR2 ligand [42]. At variance with F2L, humanin inhibits angiogenesis by modulating the expression of anti-angiogenic and pro-angiogenic mediators and preventing pathological renal microvascular remodelling [43]. However, the direct effect of this FPR agonist on endothelial cells remains unknown.

The contribution of FPRs to the angiogenic process is substantiated by the capacity of the FPR2 agonist SAA to

induce pro-angiogenic responses in different experimental models in vitro and in vivo [44–47]. In addition, the helicobacter pylori-derived peptide Hp(2–20) upregulates VEGF production, implicating this FPR1/FPR2 ligand in the vascularization and healing processes of gastric mucosa [48]. Finally, FPRs have been involved in the angiogenic responses elicited in vitro and in vivo by the vitreous fluid isolated from patients affected by proliferative diabetic retinopathy [10]. Together, these data point to a role for FPRs in angiogenesis, even though experimental evidences are sometimes contradictory and the mechanism of action of the different FPR agonists, including their receptor selectivity, will require further investigation. Relevant to this point, D-Succ-F3 is devoid of a significant mitogenic activity for HUVECs. Thus, in keeping with the chemoattractant nature of FPRs, the pro-angiogenic activity of FPR ligands appears to depend upon their capacity to trigger a migratory response in endothelial cells, essential for sprouting angiogenesis [49]. Notably, other pro-angiogenic mediators, including angiopoietin-1 and CCL2, CCL11, and CCL15 chemokines, are able to induce neovessel formation in different in vivo assays by stimulating endothelial cell migration despite their limited ability to activate mitogenic responses in these cells [50–53].

Insufficient vascularization limits size and complexity of the engineered tissues [41] and a number of ischemic tissue disorders would benefit from pro-angiogenic therapies [54]. Further experiments will be required to assess the therapeutic potential of FPR3 ligands, including pro-angiogenic D-Succ-F3 derivatives.

Retro-inversion is often used in linear peptides to obtain topologically similar molecules with improved stability features deriving from the presence of protease resistant D-amino acids [22, 23]. In our specific case, FLFLF is a palindromic sequence; thus, D-F3 and D-BOC2 peptides are the D-enantiomers of the corresponding L counterparts and, at the same time, they represent their "retro-inverso" variants. Taking advantage of the pseudo-symmetry occurring in the FLFLF sequence and the possible role played by the C-terminal carboxyl group in engaging the heparin-binding region of angiogenic growth factors [9], we generated and tested the Succ-D-F3 variant where symmetry is further enhanced by the presence of a second carboxyl moiety on the N-terminal side of the molecule. The improved symmetry would provide the peptide with the possibility to access its target in at least two quasi-equivalent orientations, thus conferring a potentially increased activity to the molecule. Comparative data obtained with the various peptides having different chirality and N-terminal groups suggest that all-L and all-D variants have orthogonal activities on VEGF- vs FPR3-mediated angiogenic responses. Indeed, the peptides of the all-L series (L-BOC2, L-F3, Succ-L-F3) suppress angiogenesis by binding and inhibiting VEGF and other heparin-binding angiogenic factors [9], whereas the corresponding D enantiomers induce angiogenesis via FPR3 with no effect on the VEGF/VEGFR2 axis. This observation suggests that the chirality of these molecules has a tremendous impact on the exposed chemical groups and surfaces used to interact with the accepting targets. In addition, we found that the N-terminally free and succinimidylated peptides have a potency significantly higher than that shown by D-BOC2. This indicates that the N-terminal charge, opposed in the two most active peptides, has a limited role in receptor recognition and that the Boc group might disturb the interaction with FPR3 by sterically interfering with its recognition.

Thus far, most of the pro-angiogenic peptides are growth factor mimetics that target their cognate receptors. For instance, various pro-angiogenic peptides have been characterized as fibroblast growth factor, angiopoietin-1, platelet growth factor or VEGF mimetics [55–57]. Here, we describe D-Succ-F3 as a novel five-amino-acid-long, pro-angiogenic D-peptide able to induce neovascular responses in various experimental settings. Its pro-angiogenic potential appears to be related to its ability to bind and activate FPR3 on the endothelial cell surface, thus shedding a new light on the biological function of this chemoattractant receptor.

Acknowledgements This work was supported in part by Associazione Italiana per la Ricerca sul Cancro (IG AIRC Grant n° 18493) to M.P and by Regione Campania, Italy [Grant "Fighting Cancer resistance: Multidisciplinary integrated Platform for a technological Innovative Approach to Oncotherapies (Campania Oncotherapies)"; Grant "Development of novel therapeutic approaches for treatment-resistant neoplastic diseases (SATIN)"; Grant NANOfotonica per la lotta al CANcro (NANOCAN)] to M.R.; S.R. was supported by an AIRC fellowship.

Author contributions Conceptualization: MIN, MP; Formal analysis and investigation: MIN, SR, CT, DC, MB, SM, MC, AS, AC; Writing—original draft preparation: MIN, MR, MP; Writing—review and editing: MP; Funding acquisition: MP, MR; Supervision: MP.

References

1. Prevete N, Liotti F, Marone G, Melillo RM, de Paulis A (2015) Formyl peptide receptors at the interface of inflammation, angiogenesis and tumor growth. Pharmacol Res 102:184–191
2. He HQ, Ye RD (2017) The formyl peptide receptors: diversity of ligands and mechanism for recognition. Molecules 22:E455
3. Ye RD, Boulay F, Wang JM, Dahlgren C, Gerard C, Parmentier M, Serhan CN, Murphy PM (2009) International union of basic and clinical pharmacology. LXXIII. Nomenclature for the formyl peptide receptor (FPR) family. Pharmacol Rev 61:119–161
4. Dorward DA, Lucas CD, Chapman GB, Haslett C, Dhaliwal K, Rossi AG (2015) The role of formylated peptides and formyl peptide receptor 1 in governing neutrophil function during acute inflammation. Am J Pathol 185:1172–1184
5. Migeotte I, Riboldi E, Franssen JD, Gregoire F, Loison C, Wittamer V, Detheux M, Robberecht P, Costagliola S, Vassart G, Sozzani S, Parmentier M, Communi D (2005) Identification and

characterization of an endogenous chemotactic ligand specific for FPRL2. J Exp Med 201:83–93
6. Harada M, Habata Y, Hosoya M, Nishi K, Fujii R, Kobayashi M, Hinuma S (2004) N-Formylated humanin activates both formyl peptide receptor-like 1 and 2. Biochem Biophys Res Commun 324:255–261
7. Koczulla R, von Degenfeld G, Kupatt C, Krötz F, Zahler S, Gloe T, Issbrücker K, Unterberger P, Zaiou M, Lebherz C, Karl A, Raake P, Pfosser A, Boekstegers P, Welsch U, Hiemstra PS, Vogelmeier C, Gallo RL, Clauss M, Bals R (2003) An angiogenic role for the human peptide antibiotic LL-37/hCAP-18. J Clin Investig 111:1665–1672
8. Lee HY, Kim SD, Shim JW, Yun J, Kim K, Bae YS (2009) Activation of formyl peptide receptor like-1 by serum amyloid A induces CCL2 production in human umbilical vein endothelial cells. Biochem Biophys Res Commun 380:313–317
9. Nawaz IM, Chiodelli P, Rezzola S, Paganini G, Corsini M, Lodola A, Di Ianni A, Mor M, Presta M (2018) N-tert-butyloxycarbonyl-Phe-Leu-Phe-Leu-Phe (BOC2) inhibits the angiogenic activity of heparin-binding growth factors. Angiogenesis 21:47–59
10. Rezzola S, Corsini M, Chiodelli P, Cancarini A, Nawaz IM, Coltrini D, Mitola S, Ronca R, Belleri M, Lista L, Rusciano D, De Rosa M, Pavone V, Semeraro F, Presta M (2017) Inflammation and N-formyl peptide receptors mediate the angiogenic activity of human vitreous humour in proliferative diabetic retinopathy. Diabetologia 60:719–728
11. Ma Y, Tao Y, Lu Q, Jiang YR (2011) Intraocular expression of serum amyloid a and interleukin-6 in proliferative diabetic retinopathy. Am J Ophtalmol 152:678–685
12. Feng J, Zhao T, Zhang Y, Ma Y, Jiang Y (2013) Differences in aqueous concentrations of cytokines in macular edema secondary to branch and central retinal vein occlusion. PLoS ONE 8:e68149
13. Wen J, Jiang Y, Zheng X, Zhou Y (2015) Six-month changes in cytokine levels after intravitreal bevacizumab injection for diabetic macular oedema and macular oedema due to central retinal vein occlusion. Br J Ophthalmol 99:1334–1340
14. Freer RJ, Day AR, Radding JA, Schiffmann E, Aswanikumar S, Showell HJ, Becker EL (1980) Further studies on the structural requirements for synthetic peptide chemoattractants. Biochemistry 19:2404–2410
15. Toniolo C, Bonora GM, Showell H, Freer RJ, Becker EL (1984) Structural requirements for formyl homooligopeptide chemoattractants. Biochemistry 23:698–704
16. Lee HY, Lee M, Bae YS (2017) Formyl peptide receptors in cellular differentiation and inflammatory diseases. J Cell Biochem 118:1300–1307
17. Schiffmann E, Aswanikumar S, Venkatasubramanian K, Corcoran BA, Pert CB, Brown J, Gross E, Day AR, Freer RJ, Showell AH, Becker EL (1980) Some characteristics of the neutrophil receptor for chemotactic peptides. FEBS Lett 117:1–7
18. Lau JL, Dunn MK (2018) Therapeutic peptides: Historical perspectives, current development trends, and future directions. Bioorg Med Chem 26:2700–2707
19. Feng Z, Xu B (2016) Inspiration from the mirror: D-amino acid containing peptides in biomedical approaches. Biomol Concepts 7:179–187
20. Milton RC, Milton SC, Kent SB (1992) Total chemical synthesis of a D-enzyme: the enantiomers of HIV-1 protease show reciprocal chiral substrate specificity [corrected]. Science 256:1445–1448
21. Schumacher TN, Mayr LM, Minor DL Jr, Milhollen MA, Burgess MW, Kim PS (1996) Identification of D-peptide ligands through mirror-image phage display. Science 271:1854–1857
22. Chorev M, Goodman M (1995) Recent developments in retro peptides and proteins–an ongoing topochemical exploration. Trends Biotechnol 13:438–445
23. Rai J (2019) Peptide and protein mimetics by retro and retroinverso analogs. Chem Biol Drug Des 93:724–736
24. Ruvo M, Fassina G (1995) End-group modified retro-inverso isomers of tripeptide oxytocin analogues: binding to neurophysin II and enhancement of its self-association properties. Int J Pept Protein Res 45:356–365
25. Eissler S, Kley M, Bachle D, Loidl G, Meier T, Samson D (2017) Substitution determination of Fmoc-substituted resins at different wavelengths. J Pept Sci 23:757–762
26. Caporale A, Doti N, Sandomenico A, Ruvo M (2017) Evaluation of combined use of Oxyma and HATU in aggregating peptide sequences. J Pept Sci 23:272–281
27. Crampton SP, Davis J, Hughes CC (2007) Isolation of human umbilical vein endothelial cells (HUVEC). J Vis Exp 3:e183
28. Coltrini D, Di Salle E, Ronca R, Belleri M, Testini C, Presta M (2013) Matrigel plug assay: evaluation of the angiogenic response by reverse transcription-quantitative PCR. Angiogenesis 16:469–477
29. Rezzola S, Nawaz IM, Cancarini A, Ravelli C, Calza S, Semeraro F, Presta M (2017) 3D endothelial cell spheroid/human vitreous humor assay for the characterization of anti-angiogenic inhibitors for the treatment of proliferative diabetic retinopathy. Angiogenesis 20:629–640
30. Varinska L, van Wijhe M, Belleri M, Mitola S, Perjesi P, Presta M, Koolwijk P, Ivanova L, Mojzis J (2012) Anti-angiogenic activity of the flavonoid precursor 4-hydroxychalcone. Eur J Pharmacol 691:125–133
31. Goodwin AM (2007) In vitro assays of angiogenesis for assessment of angiogenic and anti-angiogenic agents. Microvasc Res 74:172–183
32. Belleri M, Ronca R, Coltrini D, Nico B, Ribatti D, Poliani PL, Giacomini A, Alessi P, Marchesini S, Santos MB, Bongarzone ER, Presta M (2013) Inhibition of angiogenesis by β-galactosylceramidase deficiency in globoid cell leukodystrophy. Brain 136:2859–2875
33. Mitola S, Moroni E, Ravelli C, Andres G, Belleri M, Presta M (2008) Angiopoietin-1 mediates the proangiogenic activity of the bone morphogenic protein antagonist Drm. Blood 112:1154–1157
34. Monte W (1995) The zebrafish book. A guide for the laboratory use of zebrafish (Danio rerio). University of Oregon Press, Eugene
35. Nicoli S, De Sena G, Presta M (2009) Fibroblast growth factor 2-induced angiogenesis in zebrafish: the zebrafish yolk membrane (ZFYM) angiogenesis assay. J Cell Mol Med 13:2061–2068
36. Wang B, Shen J, Wang Z, Liu J, Ning Z, Hu M (2018) Isomangiferin, a novel potent vascular endothelial growth factor receptor 2 kinase inhibitor, suppresses breast cancer growth, metastasis and angiogenesis. J Breast Cancer 21:11–20
37. Rezzola S, Dal Monte M, Belleri M, Bugatti A, Chiodelli P, Corsini M, Cammalleri M, Cancarini A, Morbidelli L, Oreste P, Bagnoli P, Semeraro F, Presta M (2015) Therapeutic potential of anti-angiogenic multitarget N, O-sulfated *E. coli* K5 polysaccharide in diabetic retinopathy. Diabetes 64:2581–2592
38. Bae YS, Lee HY, Jo EJ, Kim JI, Kang HK, Ye RD, Kwak JY, Ryu SH (2004) Identification of peptides that antagonize formyl peptide receptor-like 1-mediated signaling. J Immunol 173:607–614
39. Shin EH, Lee HY, Kim SD, Jo SH, Kim MK, Park KS, Lee H, Bae YS (2006) Trp-Arg-Trp-Trp-Trp-Trp antagonizes formyl peptide receptor like 2-mediated signaling. Biochem Biophys Res Commun 341:1317–1322
40. Lee SY, Lee MS, Lee HY, Kim SD, Shim JW, Jo SH, Lee JW, Kim JY, Choi YW, Baek SH, Ryu SH, Bae YS (2008) F2L, a peptide derived from heme-binding protein, inhibits LL-37-induced cell proliferation and tube formation in human umbilical vein endothelial cells. FEBS Lett 582:273–278

41. Van Hove AH, Benoit DS (2015) Depot-based delivery systems for pro-angiogenic peptides: a review. Front Bioeng Biotechnol 3:102
42. De Y, Chen Q, Schmidt AP, Anderson GM, Wang JM, Wooters J, Oppenheim JJ, Chertov O (2000) LL-37, the neutrophil granule- and epithelial cell-derived cathelicidin, utilizes formyl peptide receptor-like 1 (FPRL1) as a receptor to chemoattract human peripheral blood neutrophils, monocytes, and T cells. J Exp Med 192:1069–1074
43. Zhang X, Urbieta-Caceres VH, Eirin A, Bell CC, Crane JA, Tang H, Jordan KL, Oh YK, Zhu XY, Korsmo MJ, Bachar AR, Cohen P, Lerman A, Lerman LO (2012) Humanin prevents intra-renal microvascular remodeling and inflammation in hypercholesterolemic ApoE deficient mice. Life Sci 91:199–206
44. Lee MS, Yoo SA, Cho CS, Suh PG, Kim WU, Ryu SH (2006) Serum amyloid A binding to formyl peptide receptor-like 1 induces synovial hyperplasia and angiogenesis. J Immunol 177:5585–5594
45. Lv M, Xia YF, Li B, Liu H, Pan JY, Li BB, Zhang C, An FS (2016) Serum amyloid A stimulates vascular endothelial growth factor receptor 2 expression and angiogenesis. J Physiol Biochem 72:71–81
46. Cai X, Freedman SB, Witting PK (2013) Serum amyloid A stimulates cultured endothelial cells to migrate and proliferate: inhibition by the multikinase inhibitor BIBF1120. Clin Exp Pharmacol Physiol 40:662–670
47. O'Neill L, Rooney P, Molloy D, Connolly M, McCormick J, McCarthy G, Veale DJ, Murphy CC, Fearon U, Molloy E (2015) Regulation of inflammation and angiogenesis in giant cell arteritis by acute-phase serum amyloid A. Arthritis Rheumatol 67:2447–2456
48. de Paulis A, Prevete N, Rossi FW, Rivellese F, Salerno F, Delfino G, Liccardo B, Avilla E, Montuori N, Mascolo M, Staibano S, Melillo RM, D'Argenio G, Ricci V, Romano M, Marone G (2009) Helicobacter pylori Hp(2–20) promotes migration and proliferation of gastric epithelial cells by interacting with formyl peptide receptors in vitro and accelerates gastric mucosal healing in vivo. J Immunol 183:3761–3769
49. Lamalice L, Le Boeuf F, Huot J (2007) Endothelial cell migration during angiogenesis. Circ Res 100:782–794
50. Davis S, Aldrich TH, Jones PF, Acheson A, Compton DL, Jain V, Ryan TE, Bruno J, Radziejewski C, Maisonpierre PC, Yancopoulos GD (1996) Isolation of angiopoietin-1, a ligand for the TIE2 receptor, by secretion-trap expression cloning. Cell 87:1161–1169
51. Salcedo R, Ponce ML, Young HA, Wasserman K, Ward JM, Kleinman HK, Oppenheim JJ, Murphy WJ (2000) Human endothelial cells express CCR2 and respond to MCP-1: direct role of MCP-1 in angiogenesis and tumor progression. Blood 96:34–40
52. Salcedo R, Young HA, Ponce ML, Ward JM, Kleinman HK, Murphy WJ, Oppenheim JJ (2001) Eotaxin (CCL11) induces in vivo angiogenic responses by human CCR3+ endothelial cells. J Immunol 166:7571–7578
53. Hwang J, Kim CW, Son KN, Han KY, Lee KH, Kleinman HK, Ko J, Na DS, Kwon BS, Gho YS, Kim J (2004) Angiogenic activity of human CC chemokine CCL15 in vitro and in vivo. FEBS Lett 570:47–51
54. Petrak K, Vissapragada R, Shi S, Siddiqui Z, Kim KK, Sarkar B, Kumar VA (2019) Challenges in translating from bench to bedside: pro-angiogenic peptides for ischemia treatment. Molecules 24:1219
55. De Rosa L, Di Stasi R, D'Andrea LD (2018) Pro-angiogenic peptides in biomedicine. Arch Biochem Biophys 660:72–86
56. Selvaprithviraj V, Sankar D, Sivashanmugam A, Srinivasan S, Jayakumar R (2017) Pro-angiogenic molecules for therapeutic angiogenesis. Curr Med Chem 24:3413–3432
57. D'Andrea LD, Del Gatto A, De Rosa L, Romanelli A, Pedone C (2009) Peptides targeting angiogenesis related growth factor receptors. Curr Pharm Des 15:2414–2429